Pergamon

Int. J. Heat Mass Transfer. Vol. 38, No. 6, pp. 989–998, 1995

0017–9310/95 $9.50 + 0.00

0017–9310(94)00232–0

Level swell in pool boiling with liquid circulation

B. BOESMANS and J. BERGHMANS

K. U. Leuven, Department of Mechanical Engineering, Celestijnenlaan 300 A, B-3001 Heverlee, Belgium

(*Received* 11 *February* 1994 *and in final form* 16 *July* 1994)

Abstract—Level swell in pool boiling is overestimated by drift-flux equations for forced convection boiling. This is attributed to the presence in pool boiling of large slug-like bubbles and of bubble induced liquid circulation. These phenomena are analysed and a new drift-flux equation is presented which is specifically aimed at predicting void fraction in pool boiling. The correlation is compared to a set of experimental data and proves to be more accurate than other existing correlations.

INTRODUCTION

Boiling in a pool of stagnant liquid is known to cause a swelling liquid level, due to the large specific volume of the rising vapour bubbles compared to that of the liquid. Predictions of the amount of level swell (or the average void fraction beneath the liquid surface) are required for diverse applications of heat and mass transfer in bubble columns or pool boiling. Level swell is also of importance for the design of emergency pressure relief systems for liquefied gases, which is an item of major concern in chemical process safety [1].

In the past numerous correlations have been published for predicting the void fraction in liquid pools through which vapour is rising [2–11]. Some of these are in a format which corresponds to the drift-flux model for one-dimensional two-phase flow [12], which makes them especially suitable for inclusion in numerical two-phase flow computations. For forced convection boiling it is common practice to compute void fractions from the drift-flux equation:

$$\frac{1}{\langle\varepsilon\rangle} = C_0 + \frac{C_1}{Fr} \tag{1}$$

where Fr is defined in equation (7) and with coefficients $C_0 = 1.2$ and $C_1 = 1.41$ [13]. As shown in Fig. 1, this equation has a tendency to overestimate void fraction for pool boiling in large diameter vessels. This is attributed to its inability to account for:

- liquid circulation, arising from the density difference between vapour and liquid, which tends to concentrate vapour in regions with upward liquid velocity (Figs. 4 and 5) [5, 11];
- the presence of large fast-rising bubbles, which are unstable in flows with high liquid velocity, but which may exist in stagnant liquid pools if bubble formation allows for agglomeration of individual bubbles [14, 15].

It must be emphasized that equation (1) is very well suited for two-phase flows with non-negligible liquid velocity in small diameter tubes, such as are typically encountered in forced convection boiling. Typical pool boiling configurations (see Fig. 2) have very low liquid velocities and large diameters. Therefore pool boiling requires a specific void fraction model. Some

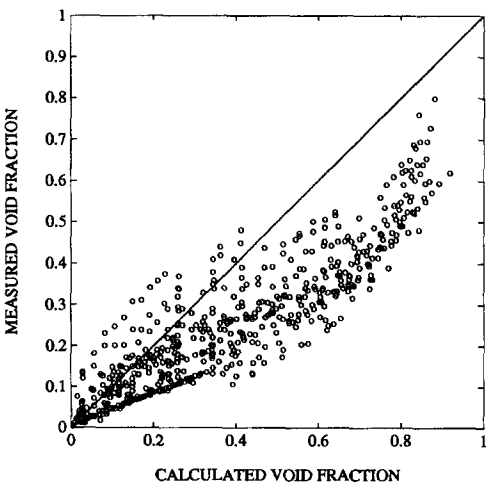

Fig. 1. Equation (1) compared to experimental data.

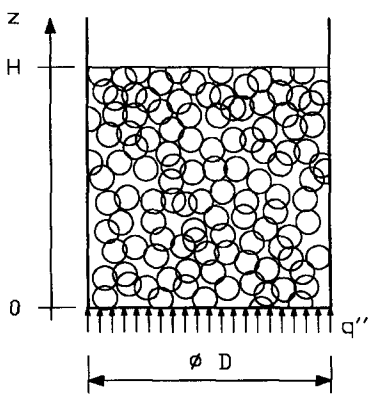

Fig. 2. Pool boiling configuration.

NOMENCLATURE

Bo $d_b^2 g\Delta\rho/\sigma$, Bond number
c heat capacity [J kg^{-1} K^{-1}]
C_0 distribution coefficient in drift-flux model
C_1 velocity coefficient in drift-flux model
C_D drag coefficient
D pool diameter [m]
D^* dimensionless pool diameter, defined in equation (32)
d_b bubble diameter [m]
F_{ci} liquid circulation factor in drift-flux model
Fr Froude number, defined in equation (7)
g gravitational acceleration [m s^{-2}]
H pool height [m]
j superficial velocity [m s^{-1}]
Ja Jakob number, $\rho_l c_l (T-T_{sat})/\rho_v \Delta h_{lv}$
k thermal conductivity [W m^{-1} K^{-1}]
K_s sphericity factor for bubble growth law
l thickness of flow reversal region [m]
n interaction coefficient in drift-flux model
P property number, $\rho_l^2\sigma^3/g\Delta\rho\mu_l^4$
$\dot{P}_{pot}$ cross-sectional release rate of mechanical energy [W m^{-1}]
$\dot{P}_{diss}$ cross-sectional dissipation rate of mechanical energy [W m^{-1}]
q'' heat flux applied to bottom of liquid pool [W m^{-2}]
r^* dimensionless bubble size, $(d_b/2)(g\rho_l\Delta\rho/\mu_l^2)^{1/3}$
R_d detachment radius [m]
v^* dimensionless bubble rise velocity, $w_\infty(\rho_l/\mu_l g\Delta\rho)^{1/3}$
V liquid circulation velocity [m s^{-1}]
w (vertical) absolute velocity [m s^{-1}]
$\tilde{w}_{vj}$ phase-averaged vapour drift velocity [m s^{-1}]
w_∞ terminal single bubble rise velocity [m s^{-1}].

Greek symbols
α thermal diffusivity [m^2 s^{-1}]
δ relative deviation, defined in equation (40)
Δ absolute deviation, defined in equation (41)
ε void fraction
μ dynamic viscosity [Pa s]
ν kinematic viscocity [m^2 s^{-1}]
ρ density [kg m^{-3}]
σ surface tension [N m^{-1}].

Subscripts and superscripts
l liquid
v vapour
1 high void fraction region
2 low void fraction region.

Operators
$\langle x \rangle$ cross-section averaged value of x
$\Delta x = x_v - x_l$.

of the published correlations, especially those developed by Kataoka and Ishii [11] and by Mersmann [7], achieve a better predictive performance, but are still completely empirical as far as the effects of liquid circulation are concerned.

In the present work a novel drift-flux type correlation is developed specifically aimed at predicting void fraction in pool boiling correlations. Due to the inclusion of a model for liquid circulation, the new correlation is consistent with existing theory related to single bubble rise velocities. Moreover the new correlation is more accurate than any of the existing correlations.

THEORY

The drift-flux model

The drift-flux model [12] relates the cross-section averaged void fraction in a cross-section of a one-dimensional two-phase flow to the volumetric fluxes of vapour and liquid:

$$\frac{1}{\langle\varepsilon\rangle} = C_0 \frac{\langle j_v + j_l \rangle}{\langle j_v \rangle} + \frac{\tilde{w}_{vj}}{\langle j_v \rangle}. \tag{2}$$

The phase-averaged drift velocity $\tilde{w}_{vj}$ was originally assumed to be equal to the rise velocity w_∞ of a single bubble in an infinite liquid pool. A more general expression which incorporates bubble interactions is

$$\tilde{w}_{vj} = w_\infty (1-\langle\varepsilon\rangle)^n. \tag{3}$$

The distribution parameter C_0 is defined by

$$\langle\varepsilon(j_v + j_l)\rangle = C_0 \langle\varepsilon\rangle \cdot \langle j_v + j_l \rangle \tag{4}$$

and is usually assumed to be close to unity. For pool boiling with vapour generation at the bottom of the liquid pool (see Fig. 2), the continuity equation requires that in every cross-section

$$\rho_v \langle j_v \rangle + \rho_l \langle j_l \rangle = 0. \tag{5}$$

Therefore the drift-flux equation becomes

$$\frac{1}{\langle\varepsilon\rangle} = C_0\left(1 - \frac{\rho_l}{\rho_v}\right) + \frac{w_\infty (1-\langle\varepsilon\rangle)^n}{\langle j_v \rangle}. \tag{6}$$

Assuming that $\rho_l \ll \rho_v$ and defining a Froude number:

$$Fr = \langle j_v \rangle \left(\frac{\rho_l^2}{\sigma g \Delta\rho}\right)^{1/4} \tag{7}$$

equation (6) can be conveniently written as

$$\frac{1}{\langle \varepsilon \rangle} = C_0 + \frac{C_1}{Fr}(1 - \langle \varepsilon \rangle)^n. \tag{8}$$

The new parameter C_1 is equal to

$$C_1 = w_\infty \left(\frac{\rho_l^2}{\sigma g \Delta\rho}\right)^{1/4} \tag{9}$$

and is a dimensionless representation of the single bubble rise velocity w_∞.

A void fraction correlation based on the drift-flux model is established by providing values for the coefficients C_0, C_1 and n, possibly depending on fluid properties.

Flow patterns in pool boiling

In bubbly flows with small liquid velocities in large diameter vessels, the following two flow patterns are observed:

- *Pure bubbly flow*—a dispersed flow in which the behaviour of individual bubbles is quite similar to that of single bubbles rising in an infinite liquid pool. An instantaneous picture of this flow pattern is nearly homogeneous, although some spatial non-uniformities, such as liquid circulation, can exist. The bubble size distribution is unimodal (all bubbles have nearly the same size) and liquid turbulence is confined to the wakes of individual bubbles;
- *Churn-turbulent flow or bubble-slug flow*—this flow is not truly dispersed but shows a chaotic and very intermittent behaviour. It is observed that fast rising large bubbles co-exist with small bubbles. The bubble size distribution is therefore bimodal, and an instantaneous picture of this flow pattern is very heterogeneous. Liquid turbulence is not confined to the bubble wakes, and its presence throughout the liquid phase guarantees a nearly uniform flow field when averaged over a sufficiently long time.

The presence of large, fast rising bubbles is a distinctive feature of churn-turbulent flow in pool boiling. They arise from the coalescence of small bubbles close to the bottom of the pool. These large bubbles are not stable in forced convection boiling, because of its high degree of liquid turbulence.

The distinction between pure bubbly and churn-turbulent flow is also made in forced convection boiling. In pool boiling the transition cannot be as clearly defined as in forced convection boiling, but generally occurs between $\langle \varepsilon \rangle = 0.25$ and $\langle \varepsilon \rangle = 0.4$. If coalescence is responsible for the presence of large bubbles, it is likely that the transition occurs at a fixed value of the Froude number Fr. For small vapour flow rates, the vapour generated at the pool bottom, forms small bubbles. For high vapour flow rates these bubbles do not rise fast enough and are overtaken by their successors and form fast-rising, large bubbles. Clearly coalescence of bubbles occurs if the vapour flow rate is high compared to the rise velocity of small bubbles, i.e. at a certain value of the Froude number. Mersmann shows [7] that coalescence of bubbles generally occurs if

$$Fr \geqslant 0.5. \tag{10}$$

This criterion is used here to mark the transition from pure bubbly to churn-turbulent flow in pool boiling.

Single bubble rise velocity

The terminal velocity of a single bubble rising in an infinite liquid pool depends on the fluid properties and on the bubble size. An excellent review on this subject has been given by Wallis [14], and is summarized here in Table 1.

The original format $v^* = f(r^*, P)$ is most useful when viscous effects dominate drag (i.e. for small bubble sizes). When inertial effects dominate the drag force, the alternative format $C_1 = f(Bo, P)$ presented here is more suitable. This is illustrated in Fig. 3.

For pure bubbly flow, the bubble size is governed by detachment mechanisms, and can for instance be computed according to equation [16]:

$$R_d = 3\left(\frac{K_s^4}{\pi^2}\frac{(Ja^2\,\alpha)^2}{g}\right)^{1/3} \tag{11}$$

for growth controlled ('dynamic') bubble departure on horizontal surfaces. Typical values are in the inertially controlled bubble rise regimes. Therefore the value of C_1 in the drift-flux equation should be close to 1.5 (possibly somewhat higher for small bubbles).

For churn-turbulent flow, bubbles tend to agglomerate close to the boiling surface and form large slug-like cap bubbles. The maximum bubble size is limited by the stability requirements of the vapour–liquid interface. Applying the theory presented by Kitscha and Kocamustafaogullari [17], the maximum bubble size can be calculated as

$$Bo = \left(0.0934 + 0.0614\frac{\rho^*}{1+\rho^*} - 0.048C_g^2\right)^{-1} \tag{12}$$

with

$$\rho^* = 1.37\frac{\rho_v}{\rho_l} \tag{13}$$

and C_g a constant of order unity which represents the ratio of growth time to propagation time of a disturbance of the bubble surface. Use is made of the bubble rise speed expression for the Taylor regime (R5), and of the experimental observation that the wake angle of spherical cap bubbles is close to 50°. The results of this expression are shown in Fig. 4.

For any particular value of C_g the maximum bubble size increases monotonically with $1-(\rho_v/\rho_l)$.

Table 1. Single bubble rise velocities according to ref. [14]

Regime	Size limits	$v^* = f(r^*, P)$	$C_1 = f(Bo, P)$
R1	$r^* < 1.5$	$v^* = \frac{1}{3}r^{*2}$	$C_1 = 0.0833 Bo\ P^{0.25}$
R2A	$1.5 < r^* < 13.4$	$v^* = 0.408 r^{*1.5}$	$C_1 = 0.1442 Bo^{0.75}\ P^{0.17}$
R2B	$13.4 < r^*$	$v^* = \frac{1}{9}r^{*2}$	$C_1 = 0.0278 Bo\ P^{0.25}$
R3	$Bo < 4$	$v^* = \sqrt{2} r^{*-1/2} P^{1/6}$	$C_1 = 2 Bo^{-0.25}$
R4	$4 < Bo < 16$	$v^* = \sqrt{2} P^{1/12}$	$C_1 = 1.414$
R5	$16 < Bo$	$v^* = r^{*1/2}$	$C_1 = 0.707 Bo^{0.25}$

Maximum bubble sizes observed in reality are close to $Bo = 400$ for $(\rho_v/\rho_l) \to \infty$ (corresponding to $C_1 \approx 3$ according to Table 1). Therefore C_1 is expected to vary between 1.5 and 3, depending on the value of $1-(\rho_v/\rho_l)$.

Bubble interactions

When a cloud of bubbles is rising through a liquid pool, their rise velocity can be significantly different from the single bubble rise velocity due to bubble interactions. These are represented in the drift-flux model via the exponent n.

For a dispersed two-phase flow, such as the pure bubbly flow, a value for n can be obtained from the two-phase momentum balance equations. Following Kataoka and Ishii [11], one obtains

$$\tilde{w}_{vj} = w_\infty \left(\frac{C_{D\infty}}{C_D}\right)^{1/2} (1 - \langle\!\langle \varepsilon \rangle\!\rangle)^{3/2}. \tag{14}$$

Here $C_{D\infty}$ is the drag coefficient of a bubble with the same dimensions as the actual bubbles, when rising in an infinitely extended liquid. It is often assumed that the drag coefficient C_D in a bubble cloud equals $C_{D\infty}$. This assumption is justified for pure bubbly flow but not necessarily for churn-turbulent flow.

It must be noted that for bubbly flow the exact value of n hardly matters. The error due to using $n = 0$ instead of $n = 3/2$ is small and probably much smaller than the inevitable error due to the variability of the bubble size. Therefore interactions in bubbly flow are neglected here and it is assumed that $n \approx 0$.

For churn-turbulent flow the drag force results mainly from dissipation in the wake of large bubbles. At higher void fractions the wake size is limited by the available space between adjacent bubbles. It is assumed that the wake length is proportional to the bubble size:

$$l_\infty \sim d_b \tag{15}$$

for non-interacting bubbles, and to the distance between neighbouring bubbles, otherwise

$$l \sim d_b \frac{1 - \langle\!\langle \varepsilon \rangle\!\rangle}{\langle\!\langle \varepsilon \rangle\!\rangle}. \tag{16}$$

Assuming that the dissipation and the drag force are proportional to the wake length, then the following expression is yielded instead of equation (14):

$$w_{vj} \sim w_\infty (1 - \langle\!\langle \varepsilon \rangle\!\rangle) \sqrt{\langle\!\langle \varepsilon \rangle\!\rangle}. \tag{17}$$

For void fractions between $\langle\!\langle \varepsilon \rangle\!\rangle = 0.3$ and $\langle\!\langle \varepsilon \rangle\!\rangle = 0.6$ the interaction factor varies only slightly. Therefore in churn-turbulent flow the use of $n = 0$ is justified.

Liquid circulation

The distribution coefficient C_0 of the drift-flux model is usually given a value between 1 and 1.5, based on a theoretical analysis by Zuber and Findlay [12], valid if both liquid and vapour are flowing in the same direction at every point of the cross-section. This is not always the case in pool boiling configurations, where liquid circulation may exist. Liquid circulation

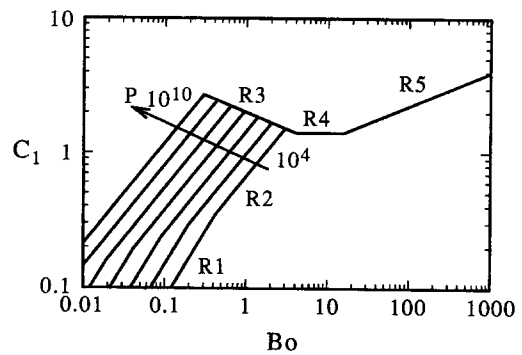

Fig. 3. Single bubble rise velocities according to ref. [14].

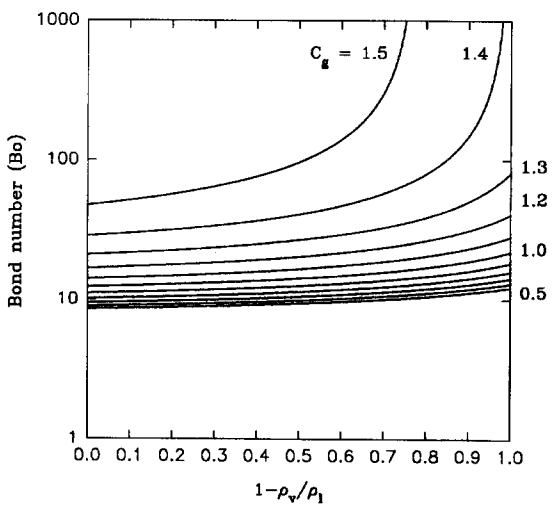

Fig. 4. Maximum size of spherical cap bubble.

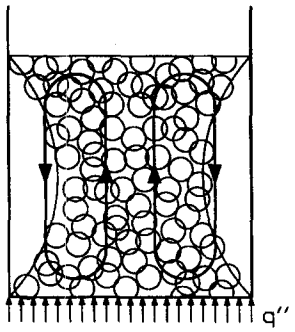

Fig. 5. Flow pattern with liquid circulation in pool boiling with vapour generation at the bottom of the pool.

can increase the value of the distribution coefficient to values between 3 and 4.

When many bubbles are rising in a liquid pool, the cross-section averaged liquid flow rate is zero, but nevertheless it is possible that a flow pattern exists in which liquid is moving upward in a region with high void fraction, and downward in a region with low void fraction (see Fig. 5).

Due to the liquid circulation potential energy is being released, because a light two-phase mixture is moving upward relative to a heavier mixture. This release of potential energy is driving the circulating flow and is balanced by the dissipation caused by viscous or turbulent shear stresses.

If the energy dissipation is small, the circulation rate can increase until all bubbles are concentrated in the high void fraction region. This occurs when the downward liquid velocity in the low void fraction region equals the single bubble rise velocity. At this circulation rate it is impossible for a single bubble to rise through the low void fraction region. At a slightly higher circulation rate vapour would be carried downward in this region and would thus prohibit a further increase of the circulation rate.

For the special case of liquid circulation at the maximum rate, and for an idealized flow pattern with upward liquid flow in the central region and downward liquid flow in the outer region, it is possible to derive an analytical expression for C_0. It is assumed that the void fraction in the central region is higher than in the outer region, and that all velocity and void fraction profiles are flat.† Furthermore an 'infinite tube' is assumed, i.e. $D/H \approx 0$ (Fig. 6).

For this idealized flow C_0 can be readily calculated from its definition as

$$C_0 = 1 + K\frac{\Delta\varepsilon}{\langle\varepsilon\rangle} \tag{18}$$

with

$$K = k(1-k)\frac{\Delta F + \dfrac{v}{w_\infty}\left(1+\dfrac{k}{1-k}\dfrac{1-\varepsilon_1}{1-\varepsilon_2}\right)}{F + \dfrac{v}{w_\infty}k\left(1-\dfrac{1-\varepsilon_1}{1-\varepsilon_2}\right)} \tag{19}$$

$$\Delta F = \frac{\varepsilon_1}{1-\varepsilon_1} - \frac{\varepsilon_2}{1-\varepsilon_2} \tag{20}$$

$$F = k\frac{\varepsilon_1}{1-\varepsilon_1} + (1-k)\frac{\varepsilon_2}{1-\varepsilon_2} \tag{21}$$

$$\Delta\varepsilon = \varepsilon_1 - \varepsilon_2 \tag{22}$$

$$\langle\varepsilon\rangle = k\varepsilon_1 + (1-k)\varepsilon_2. \tag{23}$$

At the maximum circulation rate, all vapour is concentrated in the central part of the tube and therefore

$$\varepsilon_1 = \langle\varepsilon\rangle/k \tag{24}$$

$$\varepsilon_2 = 0. \tag{25}$$

The downward liquid velocity in the outer part equals the single bubble rise velocity if

$$\frac{V}{w_\infty} = \frac{k}{k-\langle\varepsilon\rangle}. \tag{26}$$

Then the circulation coefficient becomes

$$C_0 = 1 + \frac{1}{2k}\left(1+\frac{1-2k}{k}\langle\varepsilon\rangle\right) = \frac{1}{2k} + \frac{1}{2\langle\varepsilon\rangle}. \tag{27}$$

Therefore the circulation coefficient can be significantly higher than the typical values for forced convection boiling ($C_0 = 1 \ldots 1.4$).

It is important to note that the circulation coefficient of the drift-flux model is not a constant, but depends on the average void fraction $\langle\varepsilon\rangle$. It should also be remarked that liquid circulation at the maximum rate is meaningless for $\langle\varepsilon\rangle$ greater than 0.5.

Whether or not liquid circulation can reach its maximum value is determined by the balance between the release of potential energy and the dissipation of the released energy. From dimensional analysis it can be seen that the cross-sectional release rate of potential energy due to liquid circulation scales as

$$\dot{P}_{\text{pot}} \sim g\Delta\rho D^2 V f(\langle\varepsilon\rangle, k). \tag{28}$$

The dissipation of energy is mainly confined to the high shear region close to the flow reversal point. Assuming that turbulent stresses are much larger than viscous stresses, the cross-sectional dissipation rate scales as

$$\dot{P}_{\text{diss}} \sim \rho_l D V^3 f(\langle\varepsilon\rangle, k). \tag{29}$$

Because $\dot{P}_{\text{pot}}$ and $\dot{P}_{\text{diss}}$ must be of the same order-of-magnitude, the circulation rate scales as

$$\frac{V}{w_\infty} \sim \frac{\sqrt{g\dfrac{\Delta\rho}{\rho_l}D}}{w_\infty} f(\langle\varepsilon\rangle, k). \tag{30}$$

† The assumption about the flow direction is only made for ease of understanding; the analysis is equally valid for a flow pattern with downward flow in the central region and upward flow in the outer region.

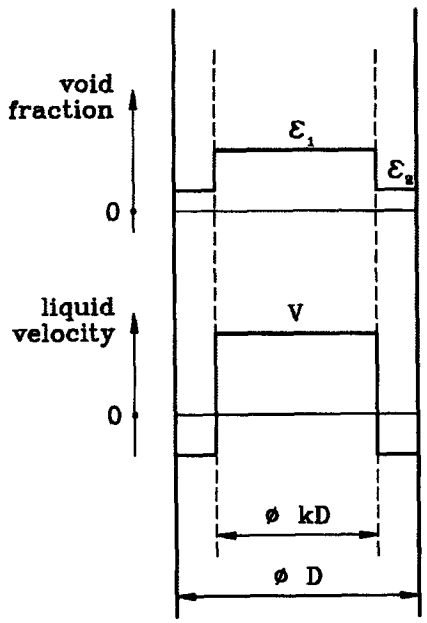

Fig. 6. Idealized flow pattern with liquid circulation in infinite tube.

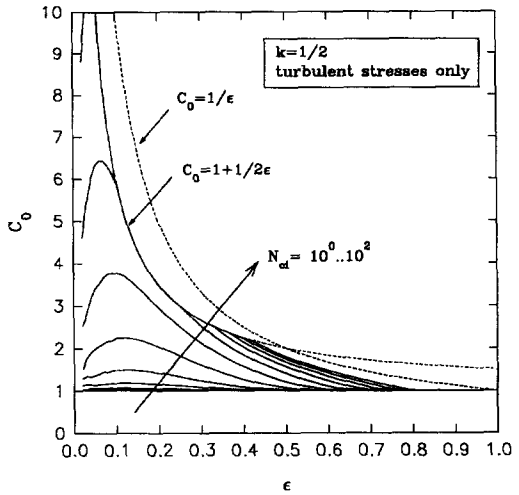

Fig. 7. Distribution coefficient with liquid circulation.

Maximum circulation [defined by equation (26)] therefore occurs at a certain value (of order unity) of the dimensionless ratio:

$$N_{ci} = \frac{\sqrt{g\frac{\Delta\rho}{\rho_l}D}}{w_\infty} = \frac{D^{*1/2}}{C_1} \tag{31}$$

where the dimensionless vessel diameter D^* is defined as

$$D^* = \frac{D}{\sqrt{\frac{\sigma}{g\Delta\rho}}}. \tag{32}$$

Liquid circulation is impossible for $N_{ci} \to 0$, and increases when N_{ci} increases until the maximum circulation rate is reached.

It should be noted that C_1 is nearly constant and can be neglected for the purposes of this scale analysis. The circulation rate is therefore determined by D^* only.

The validity of the assumption that dissipation is dominated by turbulent stresses limits the applicability of this theory to low viscosity liquids. When both viscous and turbulent dissipation are considered, the balance between potential energy release and dissipation reads

$$\left(\frac{V}{w_\infty}\right)^2\left[1+\frac{v_l}{lV}\right] \sim \frac{D^{*2}}{C_1} \tag{33}$$

where l represents the thickness of the flow reversal region in which a non-zero velocity gradient exists. Assuming that the viscous term is small but not negligible yields a first-order solution for the effect of viscous stresses:

$$\frac{V}{w_\infty} \sim \frac{\sqrt{g\frac{\Delta\rho}{\rho_l}D}}{w_\infty} \frac{1}{\sqrt{1+\frac{1}{\left(\frac{1}{D}\right)P^{1/4}D^{*3/2}}}}. \tag{34}$$

Therefore viscous dissipation can be safely neglected if $P^{1/4}D^{*3/2}$ is sufficiently large.

A somewhat more detailed numerical analysis of liquid circulation in bubble columns is presented in ref. [18]. The results which are shown in Fig. 7 are in agreement with the simple theory for maximum circulation presented here, except for very small void fractions, where the actual value of C_0 depends on N_{ci}. For void fractions around $\langle\varepsilon\rangle = 0.5$ the simple model slightly underpredicts C_0 compared to the detailed computations.

Drift-flux model for pool boiling

Although the circulation model presented here is simple, it provides valuable insight into the effect of liquid circulation on the drift-flux equation. When liquid circulation is taken into account the distribution coefficient of the drift-flux model should depend on the average void fraction according to equation (27). Substituting this expression for C_0 in the drift-flux equation (8) for pool boiling yields

$$\frac{1}{\langle\varepsilon\rangle} = \frac{1}{2k} + \frac{1}{2\langle\varepsilon\rangle} + \frac{C_1}{Fr}(1-\langle\varepsilon\rangle)^n \tag{35}$$

which is equivalent to

$$\frac{1}{\langle\varepsilon\rangle} = \frac{1}{k} + 2\frac{C_1}{Fr}(1-\langle\varepsilon\rangle)^n. \tag{36}$$

Therefore liquid circulation at the maximum rate has

the effect of *apparently* doubling the value of C_1 in the drift-flux model if a constant C_0 is imposed.

To include the effect of liquid circulation, it is proposed here to use an extended drift-flux equation:

$$\frac{1}{\langle\varepsilon\rangle} = C_0 + F_{ci}\frac{C_1}{Fr}(1-\langle\varepsilon\rangle)^n \qquad (37)$$

with a factor F_{ci} close to $F_{ci} = 2$ if liquid circulation at the maximum rate is possible.

DATA ANALYSIS

Void fraction data

The theory presented in the previous section provides the framework for establishing a drift-flux type void fraction correlation based on experimental data. Experimental measurements of the average void fraction in vertical bubbly flow have been reported by many authors (see Table 2). For the present work, the same data set was used as in ref. [11], together with void fraction data published in graphical form by Akita and Yoshida [8] and by Wilkinson and Van Dierendanck [25]. For establishing a void fraction correlation, only those measurements are considered for which $D^* > 30$ (to exclude slug flow), $D/H \leqslant 0.2$ (long tubes), and for which the net liquid velocity is zero or sufficiently small. The shallow pool data obtained by Gonzales and Corradini [24] and Margulova [21] are only used for an *a posteriori* evaluation of the influence of the pool aspect ratio.

The complete set of data covers a range of fluid properties between

$$4\times 10^9 < P < 1.6\times 10^{13}$$

$$0.0002 < \frac{\rho_v}{\rho_l} < 0.313$$

$$0.174 < \frac{\nu_v}{\nu_l} < 146.4$$

while tube dimensions vary between

$$30 < D^* < 407$$

$$0.04 < D/H < 1.$$

Void fractions covered by the experiments range from $\langle\varepsilon\rangle = 0$ to $\langle\varepsilon\rangle = 0.8$ for Froude numbers ranging from $Fr = 0$ to $Fr = 15.9$. The total number of data points is 611 (318 of which are obtained in long tubes).

For all data points, the value of $P^{1/4}D^{*3/2}$ is larger than 1.8×10^3. Therefore the effect of viscous dissipation on liquid circulation should be negligible. Except for the data from Margulova and Gonzales, all data are obtained in tubes with $D/H < 0.2$. The circulation number N_{ci} varies between 4 and 13. Therefore full circulation is expected for most of the data points, except at very small void fractions.

Values of $F_{ci}C_1$ obtained from the experimental data, assuming $C_0 = 1$, are shown in Fig. 8 for all data with $D/H < 0.2$. It can be seen that $F_{ci}C_1$ is close to or larger than 3, except for the data obtained by Wilkinson. It should also be noted that values as large as $F_{ci}C_1 = 8$ are present in the data, which cannot be explained by the existing theory for single bubble rise velocities, not even if maximum size cap bubbles are assumed.

Void fraction correlation

The following correlation is proposed for calculating void fraction in pool boiling configurations:

$$\frac{1}{\langle\varepsilon\rangle} = C_0 + F_{ci}\frac{C_1}{Fr} \qquad (38)$$

with

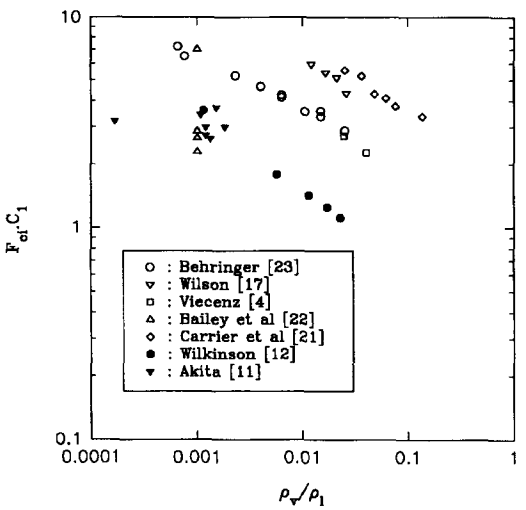

Fig. 8. Values of $F_{ci}C_1$ for long tube void fraction data.

Table 2. Sources of experimental void fraction data

Author	Fluid	Ref.	$\langle\varepsilon\rangle$	Fr
Behringer	Steam–water	[19]	0.03–0.40	0.1–4.7
Bailey	Air–water	[20]	0.11–0.62	0.2–15.9
Margulova	Steam–water	[21]	0.05–0.13	0.2–0.6
Wilson *et al.*	Steam–water	[22]	0.28–0.76	1.8–7.5
Carrier *et al.*	Steam–water	[23]	0.15–0.80	0.9–10.4
Viecenz	Freon 12	[5]	0.04–0.45	0.1–2.3
Gonzalez and Corradini	Air–different liquids	[24]	0.00–0.52	0.0–3.6
Wilkinson and Van Dierendonck	Different gases–water	[25]	0.06–0.48	0.1–1.1
Akita and Yoshida	Different gases–water Air–different liquids	[8]	0.01–0.16	0.0–1.3

Bubbly flow	$C_0 = 1.2$	$C_1 = 1.373$
Churn-turbulent flow	$C_0 = 1.2$	$C_1 = 1.373 + 0.177\left(\frac{\rho_v}{\rho_l}\right)^{-0.25}$

In general the function F_{ci} should depend on N_{ci}, but for pool boiling of low viscosity liquids it is possible to use a constant value:

$$F_{ci} = 2. \tag{39}$$

The void fraction correlation presented here covers both bubbly and churn-turbulent flow. Therefore its range of applicability should extend from pure liquid flow to void fractions of about $\langle\varepsilon\rangle = 0.6$. The set of experimental data used to establish the correlation contains data for Froude numbers ranging from 0 to $Fr = 15.9$. Equation (38) should not be used outside these limits.

It should be noted that there is a discontinuity in the void fraction given by equation (38) at the transition from pure bubbly to churn-turbulent flow. In reality the flow regime transition occurs in a transition region whose span and location are very sensitive to the presence of impurities. Experiments reveal that, in some cases, the transition region is small enough to make the transition appear like a discontinuity [13]. Unfortunately it is not possible at present to predict the conditions for this flow regime transition with great accuracy. While better models are not available, equation (10) is used here to mark the transition from bubbly to churn-turbulent flow in pool boiling.

For practical applications it is advised to consider the possibility of both bubbly flow and churn-turbulent flow for conditions close to the flow pattern transition.

The correlation coefficients in equation (38) are obtained using a Nelder–Meade non-linear optimization algorithm that minimizes the relative deviation:

$$\delta = \sqrt{\frac{1}{N}\sum_{i=1}^{N}\left(\frac{\langle\varepsilon\rangle_{exp} - \langle\varepsilon\rangle_{calc}}{\langle\varepsilon\rangle_{exp}}\right)^2} \times 100\% \tag{40}$$

between the experimental and correlated void fractions. The use of this relative deviation guarantees equal emphasis on small and large void fraction data points.

The overall performance of the void fraction correlation (38) can be judged from the parity plot shown in Fig. 9.

The average relative deviation between the correlated data and the experimental data is

$$\delta = 19\%.$$

The average absolute deviation computed as

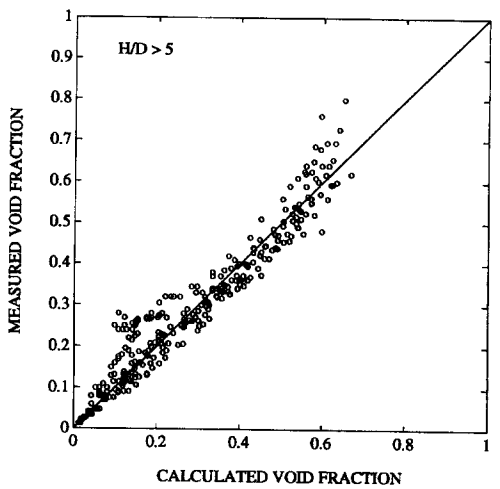

Fig. 9. Comparison between equation (38) and long tube experimental data.

$$\Delta = \sqrt{\frac{1}{N}\sum_{i=1}^{N}(\langle\varepsilon\rangle_{exp} - \langle\varepsilon\rangle_{calc})^2} \tag{41}$$

is

$$\Delta = 0.05.$$

When the correlation based on long tube data is applied to the entire data set (including shallow pools), the average relative deviation is $\delta = 34\%$ and the average absolute deviation is $\Delta = 0.08$. From the

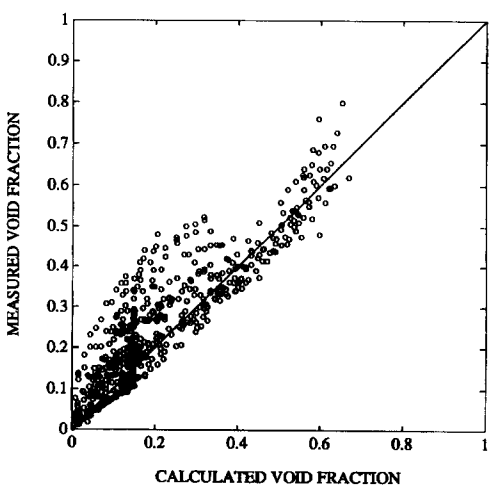

Fig. 10. Comparison between equation (38) and all experimental data.

Table 3. Comparison of void fraction correlations

Author	Correlation form	δ† [%]	Δ†	δ [%]	Δ
Kurbatov [2]	$\frac{1}{\langle\varepsilon\rangle} = 1.49 Fr^{-2/3}\left(\frac{\nu_v}{\nu_l}\right)^{2/9} D^{*1/6}$	45	0.072	49	0.091
Sterman [3]	$\frac{1}{\langle\varepsilon\rangle} = C Fr^{-2a}\left(\frac{\rho_l}{\Delta\rho}\right)^{a}\left(\frac{\rho_v}{\Delta\rho}\right)^{-0.17} D^{*0.25}$	35	0.076	49	0.117
Wilson *et al.* [4]	$\frac{1}{\langle\varepsilon\rangle} = C Fr^{-2a}\left(\frac{\rho_l}{\Delta\rho}\right)^{a}\left(\frac{\rho_v}{\Delta\rho}\right)^{-0.17} D^{*0.1}$	26	0.061	44	0.102
Viecenz [5]	$\frac{1}{\langle\varepsilon\rangle} = C Fr^{-2a}\left(\frac{\rho_l}{\Delta\rho}\right)^{-a-0.585}\left(\frac{\nu_v}{\nu_l}\right)^{-0.256} D^{*-0.174}$	41	0.067	44	0.092
Labuntsov *et al.* [6]	$\frac{1}{\langle\varepsilon\rangle} = 1+2.1 Fr^{-1}\left(\frac{\rho_l}{\Delta\rho}\right)^{-4.8}\left(\frac{\rho_v}{\Delta\rho}\right)^{-0.2}$	44	0.087	83	0.135
Mersmann [7]	$\frac{1}{\langle\varepsilon\rangle} = 1+7.143 Fr^{-1}\left(\frac{\rho_l}{\Delta\rho}\right)^{1/3} P^{-1/24}\left(\frac{\rho_l}{\rho_v}\right)^{5/72}(1-\bar{\varepsilon})^{n}$	30	0.080	37	0.089
Akita and Yoshida [8]	$\frac{1}{\langle\varepsilon\rangle} = 1+5 Fr^{-1}\left(\frac{\rho_l}{\Delta\rho}\right)^{1/3} P^{-1/24}(1-\bar{\varepsilon})^{-3}$	26	0.078	37	0.091
Gardner [9]	$\frac{1}{\langle\varepsilon\rangle} = 1+K Fr^{-2/3}\left(\frac{\rho_v}{\rho_l}\right)^{-2m/3} P^{m/3}(1-\bar{\varepsilon})^{1/2}$	57	0.05	65	0.077
Fauske [10]	$\frac{1}{\langle\varepsilon\rangle} = 1+K Fr^{-1}\frac{(1-\bar{\varepsilon})^{n}}{(1-\bar{\varepsilon}^{m})}$	121	0.25	109	0.204
Kataoka and Ishii [11]	$\frac{1}{\langle\varepsilon\rangle} = C_0 + K Fr^{-1} D^{*a}\left(\frac{\rho_v}{\rho_l}\right)^{b} P^{-0.25c}$	24	0.062	46	0.077

† Long tube data only.

parity plot (Fig. 10), it can be seen that void fractions are underestimated for shallow pools.

Comparison to other correlations

To put the accuracy of the correlation presented here into perspective, a number of existing correlations have been compared to the same set of data that were used to establish the new correlation. The results are shown in Table 3.

For this purpose all correlations have been rewritten in the same format:

$$\frac{1}{\langle\varepsilon\rangle} = f\left(Fr, P, \frac{\rho_v}{\rho_l}, \frac{\nu_v}{\nu_l}, D^*\right). \tag{42}$$

Compared to the existing correlations, the correlation presented here is simple and yet achieves a better accuracy (both relative and absolute), even if shallow pool data are included.

CONCLUSION

Level swell in pool boiling is overestimated by drift-flux equations for forced convection boiling. This is due to the existence in pool boiling of liquid circulation and large, fast-rising bubbles.

Using a simple theoretical model, it is shown that liquid circulation at the maximum rate apparently causes a doubling of the drift velocity if a constant distribution coefficient is assumed.

Based on the theoretical model, a void fraction correlation is presented [equation (38)] which is shown to be more accurate than existing void fraction correlations for pool boiling or bubbling systems.

REFERENCES

1. H. G. Fischer, H. S. Forrest, S. S. Grossel, J. E. Huff, A. R. Muller, J. A. Noronha, D. A. Shaw and B. J. Tilley, *Emergency Relief System Design Using Diers Technology—the Design Institute for Emergency Relief Systems (Diers) Project Manual.* AIChE, New York (1992).
2. A. V. Kurbatov, The bubbling and the problem of critical loads in steam separation, *Trans. Power Inst. M. V. Molotow* (Moscow) **11** (1953) (quoted from ref. [5]).
3. L. S. Sterman, The correlation of experimental data for vapour bubbling through a liquid, *Zh. Tech. Fiz.* **26,** 1519 (1956) (quoted from ref. [5]).
4. J. F. Wilson, R. J. Grenda and J. F. Patterson, Steam volume fraction in a bubbling two-phase mixture, *Trans. Am. Nucl. Soc.* **4,** 356 (1961).
5. H. J. Viecenz, Blasenaufstieg und Phasenseparation in Behaltern bei Dampfein-leitung und Druckentlastung, Doctoral Dissertation, University of Hannover (1980).
6. D. A. Labuntsov, I. P. Kornyukin and E. A. Zakharova, Vapour concentration of a two-phase adiabatic flow in vertical ducts, *Teploenergetica* **15,** 62–67 (1968).
7. A. Mersmann, Auslegung und Massstabsvergrosserung von Blasen- und Tropfensäulen, *Chemie-Ingr-Tech.* **49,** 679–691 (1977).
8. K. Akita and F. Yoshida, Gas holdup and volumetric mass transfer coefficient in bubble columns, *Ind. Engng Chem. Process Des. Devl.* **12,** 76–80 (1973).
9. G. C. Gardner, Fractional vapour content of a liquid

pool through which vapour is bubbled, *Int. J. Multiphase Flow* **6**, 399–410 (1980).
10. Fauske and Associates Inc., Emergency relief systems for runaway chemical reactions and storage vessels: a summary of multiphase flow methods, DIERS Report FAI/83-27 (1983).
11. I. Kataoka and M. Ishii, Drift flux model for large diameter pipe and new correlation for pool void fraction, *Int. J. Heat Mass Transfer* **30**, 1927–1939 (1987).
12. N. Zuber and J. A. Findlay, Average volumetric concentration in two-phase flow systems, *ASME J. Heat Transfer* **87**, 453–468 (1965).
13. G. B. Wallis, *One-dimensional Two-phase Flow*, Chap. 9. McGraw-Hill, New York (1969).
14. G. B. Wallis, The terminal speed of single drops or bubbles in an infinite medium, *Int. J. Multiphase Flow* **1**, 491–511 (1974).
15. R. Krishna, P. M. Wilkinson and L. L. Van Dierendonck, A model for gas holdup in bubble columns incorporating the influence of gas density on flow regime transitions, *Chem. Engng Sci.* **46**, 2491–2496 (1991).
16. L. Z. Zeng, J. F. Klausner and R. Mei, A unified model for the prediction of bubble detachment diameters in boiling systems—1. Pool boiling, *Int. J. Heat Mass Transfer* **36**, 2261–2270 (1993).
17. J. Kitscha and G. Kocamustafaogullari, Breakup criteria for fluid particles, *Int. J. Multiphase Flow* **15**, 573–588 (1989).
18. B. Boesmans, Transient level swell during emergency pressure relief of liquefied gases, Doctoral Dissertation, Katholieke Universiteit Leuven (1994).
19. P. Behringer, Steiggeschwindigkeit von Dampfblasen in Kesselrohren, VDI-Forschungshef 356 (1932) (data quoted from ref. [5]).
20. R. V. Bailey, Transport of gases through liquid–gas mixtures, *Proceedings of the AIChE New Orleans Meeting*, AIChE (1956) (data quoted from ref. [12]).
21. T. H. Margulova, An experimental investigation of the relative velocity of vapour in bubbling through a layer of water at high pressure, *Trans. Power Inst. M. V. Molotow* (Moscow) **11** (1953) (data quoted from ref. [5]).
22. J. F. Wilson, R. J. Grenda and J. F. Patterson, The velocity of rising steam in a bubbling two-phase mixture, *Trans. Am. Nucl. Soc.* **5**, 151 (1962).
23. F. Carrier *et al.*, Steam separation technology under the Euratom program, Allis–Chalmers Atomic Energy Division, Report No. ACNP-63021 (1963) (data quoted from ref. [12]).
24. F. G. Gonzales and M. L. Corradini, Liquid–liquid mixing by gas injection in a pool configuration, Topical Report University of Wisconsin—Madison (1989).
25. P. M. Wilkinson and L. L. Van Dierendonck, Pressure and gas density effects on bubble break-up and gas holdup in bubble columns, *Chem. Engng Sci.* **45**, 2309–2315 (1990).